Embedding versus adhesive bonding of adapted piezoceramic modules for function-integrative thermoplastic composite structures

Werner Hufenbach, Maik Gude, Thomas Heber

Embedding versus adhesive bonding of adapted piezoceramic modules for function-integrative thermoplastic composite structures

Werner Hufenbach, Maik Gude, Thomas Heber

PII: S0266-3538(11)00133-3
DOI: 10.1016/j.compscitech.2011.03.019
Reference: CSTE 4961

To appear in: *Composites Science and Technology*

Received Date: 7 October 2010
Revised Date: 14 March 2011
Accepted Date: 17 March 2011

Please cite this article as: Hufenbach, W., Gude, M., Heber, T., Embedding versus adhesive bonding of adapted piezoceramic modules for function-integrative thermoplastic composite structures, *Composites Science and Technology* (2011), doi: 10.1016/j.compscitech.2011.03.019

Embedding versus adhesive bonding of adapted piezoceramic modules for function-integrative thermoplastic composite structures

Werner Hufenbach, Maik Gude and Thomas Heber*

Technische Universität Dresden, Institute of Lightweight Engineering and Polymer Technology (ILK), Holbeinstraße 3, 01307 Dresden, Germany
* E-mail: thomas.heber@ilk.mw.tu-dresden.de, Tel.: +49 351 463 38594, Fax: +49 351 463 38143

Abstract

Against the background of an integration of piezoceramic modules into thermoplastic composite structures the development of thermoplastic-compatible piezoceramic modules (TPM) requires the consideration of the type of module-structure-connection and module position for an optimal strain transmission. While commercially available low profile transducers are applied predominantly by adhesive bonding, TPM with thermoplastic carrier films identical to the thermoplastic matrix of the composite structure offer the possibility for a material-homogeneous integration by a hot-pressing process. The aim of the presented work is to examine the influence of an adhesive layer as well as the comparison of adhesive bonding and module integration by a hot-pressing process. Therefore a common analytic model and the Finite Element Method (FEM) is used. Particular regard is given to a maximum strain transmission between the functional module and the composite structure. For pure bending as well as for pure linear expansion the studies show the advantages of a material-homogeneous integration of function modules.

Keywords: Smart materials (A), Functional composites (A), Polymer-matrix composites (A), Isostatic pressing (E), Welding/joining (E)

1. Introduction

Fibre-reinforced composites with thermoplastic matrix systems provide a high application potential for series production because of high specific mechanical properties as well as high design freedom combined with reproducible and efficient

manufacture processes. Furthermore, the integration of additional functional components, like piezoceramic actuators or sensors, in thermoplastic composite lightweight structures enables the purposeful monitoring and manipulation of the structural behaviour. For example these function-integrative thermoplastic composites exhibit the ability for quality monitoring or active vibration and noise control applications [1-3] but also for structural applications e. g. in morphing structures and compliant mechanisms [4-7].

Previously developed plane function modules are for example the Active Fiber Composite (AFC) developed at the Massachusetts Institute of Technology (MIT) by Bent and Hagood and further developed by Continuum Photonics [8, 9], the Macro Fiber Composite (MFC) developed at NASA Langley Research Center by Wilkie, Bryant, et al [10-14] and the DuraAct, which was originally developed by the German Aerospace Center (DLR) [15-17]. These modules, whose manufacture is characterized by a high manual application effort, are typically bonded to the composite by an additional adhesive in the case of using the modules in function-integrative composite structures [12, 13, 15, 18-21]. Especially for composites with a thermoplastic matrix system the module connection by an adhesive layer can likely cause delaminations and losses in strain transfer due to compatibility problems of the connected components and a relatively low material stiffness of the adhesive.

2. Thermoplastic-compatible piezoceramic modules

With regard to a high volume production of function-integrative composite structures a transition from the above mentioned assembly-oriented to a novel technology-oriented actuator integration is necessary. Therefore thermoplastic-compatible piezoceramic modules (TPM) and dedicated manufacture and integration processes are developed, which are specially adapted for a material-homogeneous embedding of the module in the composite structure and which are suitable for a series production of function-integrative thermoplastic composites [22-24]. Fig. 1 shows the typical structure of TPM with longitudinal (d_{33}) and lateral (d_{31}) active principle.

Fig. 1. Schematic build-up of TPM with d_{33}- and d_{31}-active principle

The TPM permit the substantially coherent and homogeneous embedding in the fibre-reinforced composite by a welding technology during a hot-pressing process and thus without additional bonding efforts. Therefore the TPM contains carrier films made of thermoplastics such as polyetheretherketone (PEEK) or polyamide (PA), respectively. Consequently, the thermoplastic carrier film and the matrix material of the fibre-reinforced thermoplastic composite are from the same material. As an active layer a piezoceramic wafer or piezoceramic fibres, also embedded in the respective thermoplastic matrix system, are used. When using the d_{33}-active principle, similar to the MFC concept the active layer is provided with interdigitated electrodes (IDE) to supply an electric voltage. In the case of the d_{31}-active principle a piezoceramic layer with plane electrodes in combination with a contacting interface, applied to the carrier films, is used. The main difference of the TPM in comparison to the MFC is its process adapted material design and its manufacture by use of an adapted hot pressing technique, which is suitable for series production and exhibits a material homogeneous bonding of the novel TPM to a thermoplastic composite structure without an interfering adhesive layer. Thus a very close hot melt bonding of structure and active piezoceramic layer is generated (Fig. 2).

Fig. 2. Cross section comparison of fibre-reinforced polymer structure with bonded MFC and TPM applied by hot pressing technique (s - structure, p - active piezoceramic layer, a - adhesive layer, c - polyimide film, t - thermoplastic film)

Subsequently, the difference between the connection by an adhesive layer and the material-homogeneous connection of TPM and structure with regard to the strain transmission is investigated by means of analytical and numerical calculations.

3. Comparison of material-homogeneous embedded and adhesive bonded TPM

For the investigation of the adhesive layer influence at first a geometry model of a structural beam with TPM positioned on the top and on the bottom is used as shown in Fig. 3. In reality an adhesive layer is only used in the case of incompatibility of the composite structure matrix with the thermoplastic TPM carrier film, e. g. the composite structure matrix consists of thermosetting polymers.

The analytic calculation of the induced strains takes place predominantly on the basis of the Bernoulli-Euler model, which emanates from constant strains ε_T and ε_S over TPM thickness d_T and structure thickness d_S for the case of the linear expansion and from a linear variable strain of the structure ε_S over the structure thickness for the bending case. The load application is effected by inducing an electric field in the TPM and a resulting constant actuation strain ε_A for free TPM. It is assumed that the TPM react to the admission of a positive and/or negative electrical operating voltage with a constant positive and/or negative actuation strain of the same absolute value. Consequently for inducing a pure linear expansion the TPM strains ε_T are equal in absolute value and algebraic sign, whereas the signs are different for the bending case.

Fig. 3. Beam model with adhesive bonded or material-homogeneous connected TPM for inducing of linear expansion (a) and bending (b)

The structure consists of fibre-reinforced thermoplastic polymer with quasi-isotropic material behaviour. It is assumed that structure and TPM are of the same thermoplastic matrix system, whereby for the case of an infinitesimal adhesive layer thickness ($d_K = 0\,\mathrm{mm}$) a material-homogeneous connection of the TPM to the structure is possible, in the following called as „perfect connection“.

The induced strain for the case of linear expansion and perfect connection follows according to the Bernoulli-Euler model [25] as

$$\varepsilon_S = \varepsilon_T = \frac{2\varepsilon_A}{2+\psi} \tag{1}$$

with the relative stiffness ratio

$$\psi = \frac{E_S A_S}{E_T A_T} = \frac{E_S b_S d_S}{E_T b_T d_T} \tag{2}$$

consisting of the modules of elasticity E_S, E_T and the cross sectional areas A_S, A_T of structure and TPM, where the particular cross sectional area is calculated from width b and thickness d.

The induced strain in the bending case for perfect connection is calculated as

$$\varepsilon_S(y) = \varepsilon_T(y) = \frac{2E_T A_T \left(\frac{d_S}{2} + \frac{d_T}{2} \right) \varepsilon_A}{E_S \frac{b_S d_S^3}{12} + 2E_T I_T} y \tag{3}$$

with the moment of inertia for a TPM

$$I_T = A_T \left(\frac{d_S^2}{4} + \frac{d_S d_T}{2} + \frac{d_T^2}{3} \right). \tag{4}$$

Under consideration of a finite adhesive layer thickness the induced strains in the TPM and the structure result in the case of linear expansion according to the Bernoulli-Euler model as

$$\varepsilon_T = \frac{2}{2+\psi} \left(1 + \frac{\psi}{2} \frac{\cosh(\tau_d \bar{x})}{\cosh(\tau_d)} \right) \varepsilon_A \tag{5}$$

$$\varepsilon_S = \frac{2}{2+\psi} \left(1 - \frac{\cosh(\tau_d \bar{x})}{\cosh(\tau_d)} \right) \varepsilon_A \tag{6}$$

with the shear parameter

$$\tau_d = \sqrt{\frac{\frac{G_K d_K}{E_T d_T}}{\left(\frac{d_K}{l_T} \right)^2} \left(\frac{2+\psi}{\psi} \right)}, \tag{7}$$

where $\bar{x}$ is a dimensionless coordinate ($-1 \le \bar{x} \le 1$) along the TPM length l_T (compare Fig. 4) and G_K the shear modulus of the adhesive layer. By integration of equation (6) over $\bar{x} = -1$ to $\bar{x} = 1$ the entire deformation u induced into the structure results as

$$u = \frac{2}{2+\psi}\left(1 - \frac{1}{\tau_d}\tanh(\tau_d)\right) l_T \varepsilon_A . \tag{8}$$

With this equation the evaluation of the shear loss caused by the adhesive layer in comparison to the perfect connection ($\tau_d = \infty$) is possible.

The fraction of the adhesive layer in the total flexural rigidity is neglected for the bending case; the adhesive layer supplies only an additional strain fraction. Furthermore the adhesive layer is assumed as infinitely thin, so that the distance between TPM and structure is equal to zero, similar to the perfect connection. For the bending case the TPM and structural strains are expressed as

$$\varepsilon_T(y) = \left(\frac{12}{d_S} y + \psi \frac{\cosh(\tau_b \bar{x})}{\cosh(\tau_b)}\right) \frac{1 + \frac{1}{D}}{6 + \psi + \frac{12}{D} + \frac{8}{D^2}} \left(1 - \frac{\cosh(\tau_b \bar{x})}{\cosh(\tau_b)}\right) \varepsilon_A , \tag{9}$$

$$\varepsilon_S(y) = \frac{12}{d_S} y \frac{1 + \frac{1}{D}}{6 + \psi + \frac{12}{D} + \frac{8}{D^2}} \left(1 - \frac{\cosh(\tau_b \bar{x})}{\cosh(\tau_b)}\right) \varepsilon_A \tag{10}$$

with the shear parameter for bending

$$\tau_b = \sqrt{\frac{\frac{G_K d_K}{E_T d_T}}{\left(\frac{d_K}{l_T}\right)^2} \left(\frac{6 + \psi + \frac{12}{D} + \frac{8}{D^2}}{\psi\left(1 + \frac{1}{D}\right)}\right)} \tag{11}$$

and the thickness ratio between structure and TPM

$$D = \frac{d_S}{d_T}. \tag{12}$$

In the bending case the structure's curvature

$$\kappa = -\frac{2\varepsilon_S}{d_S} \tag{13}$$

induced by the actuation strain serves for the evaluation of shear loss caused by the adhesive layer, similar to the induced strain for the expansion case.
For the numeric verification of the analytic results a two-dimensional FE-model adapted to the analytic model was designed considering existing symmetries with regard to the y-coordinate with the help of ANSYS. The model, consisting of plane elements of type 223, was developed on the assumption of a plane stress state (Fig. 4). The adhesive layer was modelled with elastic properties. In order to investigate the structural influence of the adhesive layer, its thickness d_K can be specifically adapted. In case of perfect connection $d_K = 0\,\text{mm}$ is valid (e.g. in Fig. 5). Fig. 4 is presented with $d_K = 0.1\,\text{mm}$, whereupon four elements are utilized over the thickness so that shear-locking effects caused by an insufficient mesh density are excluded and the model exhibits the ability to reproduce spatial shear stress states.

Fig. 4. FE-model (half-model) for the investigation of the actuator-induced strain and bending of a structural beam

The solution of the model is made by a thermomechanical approach under utilization of the analogy between piezoelectric and thermal strains, whereas for the respective direction the coefficient of thermal expansion is replaced by the piezoelectric load constant and the temperature change is replaced by the electrical field for inducing a defined actuation strain.
Fig. 5 shows the strain of the structure ε_S normalized to the actuation strain ε_A at the structure surface under perfect connection of the TPM for linear expansion and bending as a function of the thickness ratio D. As input parameters for the computation a constant actuation strain $\varepsilon_A = 0.0015$ and TPM thickness $d_T = 0.2\,\text{mm}$ as well as

constant Young's moduli ($E_T = 30\,\text{GPa}$, $E_S = 60\,\text{GPa}$) and widths ($b_T = b_S = 20\,\text{mm}$) of structure and TPM are assumed.

Fig. 5. Structural strain as a function of the thickness ratio

With decreasing structure thickness the strain converges to the actuation strain in the case of expansion, since the structure rigidity draws near zero and the TPM can expand unhindered. In the case of induced bending however the contrary actuation strains of the TPM cancel each other when the structure thickness becomes zero. By reason that the represented analytically and numerically determined curves show a very good agreement, a sufficiently exact map of both load cases on the basis of the Bernoulli-Euler model can be assumed.

Under consideration of an adhesive layer thickness of $d_K = 0.2\,\text{mm}$ and an adhesive Young's modulus of $E_K = 1\,\text{GPa}$ as well as a constant thickness ratio of $D = 5$ the normalized strain for structure and TPM is illustrated as a function of $\bar{x}$ (Fig. 6). In the centre of the TPM ($\bar{x} = 0$) no strain loss caused by the adhesive layer can be seen for both load cases in comparison to the perfect connection. However the strain loss increases progressively with approaching the TPM edge, so that at $\bar{x} = 1$ no more actuation strain can be transferred to the structure. The analytical calculation of the TPM strain is only limited valid for the bending case, since the strain at the TPM edge converges to the actuation strain in reality and not to zero (see FE result in Fig. 6).

Fig. 6. Strain as a function of $\bar{x}$ along the TPM length for linear expansion (a) and bending (b)

For better evaluation of the shear loss caused by the adhesive layer, Fig. 7 shows the induced total deformation for the expansion case and the structure's curvature for the bending case, respectively, as a function of the adhesive layer thickness for varying Young's modulus of the adhesive. The presentation of the bending results is regarded on the position $\bar{x} = 0.8$ for a TPM length $l_T = 30\,\text{mm}$. In comparison to the optimal case of perfect connection, for both load cases an increasing adhesive layer thickness and a decreasing adhesive stiffness result in a reduction of the induced deformation and curvature, respectively.

Fig. 7. Induced deformation for pure expansion (a) and induced curvature for bending (b) as a function of adhesive layer thickness and stiffness

4. Embedding of TPM

Resulting from the hot-pressing manufacture process of function-integrative thermoplastic composites, TPM offer the possibility for material-homogeneous embedding in almost any position over the composite thickness beside the possibility of perfect connection. For the calculation of this integration case the TPM at the top and bottom of the structure will offset in the direction of the neutral plane by the TPM thickness d_T plus the embedding depth h (Fig. 8). The previously considered adhesive layer is not applicable in this case.

Fig. 8. Beam model with embedded TPM for induced expansion (a) and bending (b)

With integrated TPM the determination of the induced strain and deformation for linear expansion, respectively, is calculated by equation (1) analogue to the case of perfect connection, whereas the reduction of the structure rigidity due to the embedded TPM has to be considered. Thus the strain follows as

$$\varepsilon_S = \varepsilon_T = \frac{u}{l_T} = \frac{2\varepsilon_A}{2+\psi} \tag{14}$$

with the adapted relative stiffness ratio according to equation (2)

$$\psi = \frac{E_S A_S}{E_T A_T} = \frac{E_S\left(b_S d_S - 2b_T d_T\right)}{E_T b_T d_T}. \tag{15}$$

For the calculation of the induced strain in the bending case the moment of inertia of the structure in equation (3) has to be reduced by the moment of inertia I_T of the TPM, which are located with the distance a to the neutral plane, so that

$$\varepsilon_S(y) = \varepsilon_T(y) = -\kappa y = \frac{2E_T A_T\left(a + \frac{d_A}{2}\right)\varepsilon_A}{E_S\left(\frac{b_S d_S^3}{12} - 2I_T\right) + 2E_T I_T} y\,, \tag{16}$$

where a is calculated from the structure and TPM thickness as well as the embedding depth h as

$$a = \frac{d_S}{2} - d_T - h\,. \tag{17}$$

Under linear expansion the induced strains and deformations, respectively, are independent from the embedding depth of the TPM. Fig. 9 a compares the induced deformation of embedded TPM in the structure with the deformation in the case of perfect connection as functions of the thickness ratio of structure and TPM. The difference between the curves only results from the theoretical reduced structure rigidity due to the module cavities in integration case. If no module cavities are provided in reality, no significant reduction of the structure rigidity is observed and the deformations of the integration case converge to the deformations of perfect connection. Furthermore for the bending case Fig. 9 b shows the run of the structure curvature against the thickness ratio and embedding depth, where an embedding depth of $h = 0\,\text{mm}$ considers the congruent position of TPM and structure outer surface. Because of a constant TPM thickness of $d_T = 0{,}2\,\text{mm}$ the case of perfect connection, shown for comparison, results in an embedding depth of $h = -0{,}2\,\text{mm}$.

Fig. 9. Induced deformation for linear expansion (a) and induced structure curvature for bending (b) as a function of thickness ratio and embedding depth

With an increasing thickness ratio the induced structure curvature decreases. The maximum curvature can be reached by integrating the TPM right under the structure surface, proven by the comparison between embedding and perfect connection at a constant thickness ratio of $D = 5$. However analogue to the expansion case a reduced structure rigidity due to module cavities has to be considered.

5. Deformation energy transmission

An additional method for comparison of different TPM-structure-combinations for the considered load cases is the evaluation of the deformation energy induced in the structure. The efficiency of the deformation energy transmission

$$\eta = \frac{U_S}{U_{\max}} = \frac{\frac{1}{2}\int_S \sigma_S \varepsilon_S dV_S}{2\left(\frac{1}{2}\int_T \sigma_T \varepsilon_A dV_T\right)} = \frac{2E_S A_S l_T \frac{\varepsilon_A^2}{(2+\psi)^2}}{E_T A_T l_T \varepsilon_A^2} = \frac{2\psi}{(2+\psi)^2} \tag{18}$$

is an adequate evaluation criterion and is defined as the ratio of the deformation energy induced in the structure U_S and the maximum existent energy in the structure $U_{\max}$. The relative stiffness ratio ψ is calculated by equation (2).

On the basis of a perfect connection of structure and TPM, in Fig. 10 the efficiency of the deformation energy transmission for expansion and bending is shown under variation of the thickness ratio D and the ratio of Young's moduli E of structure and TPM. Under both load cases the increase of the Young's modulus ratio causes a shifting of the maximum deformation energy transmission to decreasing thickness ratios.

Fig. 10. Efficiency of the deformation energy transmission for linear expansion (a) and bending (b) as a function of thickness ratio and ratio of Young's moduli

6. Conclusions

Novel piezoceramic modules with adapted thermoplastic carrier films offer the advantage of a material homogeneous integration into fibre-reinforced thermoplastic composites using a welding process. For the case of bending as well as of pure linear expansion the presented calculative studies show the advantages of a material-homogeneous integration of function modules in relation to adhesive bonded modules. Due to the reduced material stiffness of an additional adhesive compared to the composite structure and the TPM, the module connection by an adhesive layer comes along with a shear loss between TPM and structure. Additionally it is to be noticed that in reality occurring adhesion problems because of the material-inhomogenously

connection of the components were not considered. Furthermore the efficiency of the deformation energy transmission can be increased for certain applications by connecting the TPM not to the outer surface, but inside the structure. Thus e. g. for the induction of a preferable large bending deformation, it is advantageous to integrate the TPM direct under the surface of the composite structure.

Acknowledgement

The authors express their thanks to the German Research Foundation (DFG) for the financial support of the investigations in the frame of the Collaborative Research Centre/Transregional Research Centre 39 (SFB/TR 39), subproject A5.

References

[1] Hufenbach W, Täger O, Dannemann M. Structural-dynamic design of the textile-reinforced composites with integrated piezo-actuators. Latest advancement of applied composite technology: SAMPE Europe 27th Int. Conf., La Salvetat-Saint Gilles: SEBO, 2006. p. 27-31.

[2] Fidali M, Kostka P, Langkamp A, Hufenbach W. Modelling of dynamic behaviour of a rotating composite disk with different levels of delamination. Opoka E (Ed.): Modelowanie w mechanice: XLVI sympozjon PTMTS, Gliwice: Wydawn, Katedry Mechaniki Stosowanej, 2007. p. 7-12.

[3] Schmidt K. Aktive Schwingungskompensation an einer PKW-Dachstruktur. Adaptronic Congress, Wolfsburg, 01-03 April 2003.

[4] Hufenbach W, Gude M, Czulak A. Actor-initiated snap-through of unsymmetric composites with multiple deformation states. Journal of Materials Processing Technology 2006; 175 1-3: 225-230.

[5] Gude M, Hufenbach W. Design of novel morphing structures based on bi-stable composites and piezoceramic actuators. Mechanics of Composite Materials 2006; 42 4: 339-346.

[6] Franitza D, Hufenbach W, Modler N, Modler K-H, Lichtneckert T. Bewegung durch Verformung – Simulation nachgiebiger Mechanismen aus thermoplastbasierten Faserverbundwerkstoffen. VDI (Ed.): Bewegungstechnik – Lösung von Bewegungsaufgaben mit Koppelgetrieben, Kurvengetrieben und

gesteuerten Antrieben im Maschinen-, Fahrzeug- und Gerätebau. Düsseldorf: VDI, 2006. p. 389-402.

[7] Modler N. Nachgiebigkeitsmechanismen aus Textilverbunden mit integrierten aktorischen Elementen. Dissertation, Technische Universität Dresden, 2008.

[8] Hagood N, Bent A. Development of Piezoelectric Fiber Composites for Structural Actuation. Proc. AIAA/ASME Structures, Structural Dynamics and Materials Conf., La Jolla, CA, 19-22 April 1993. p. 1-15

[9] Bent A. Active Fiber Composite Material Systems for Structural Control Applications. Proc. SPIE's 6th Int. Symp. on Smart Structures and Materials, Newport Beach, CA, 1-5 March 1999.

[10] Wilkie W, et al. Low-Cost Piezocomposite Actuator for Structural Control Applications. Proc. SPIE's 7th Int. Symp. on Smart Structures and Materials, Newport Beach, CA, 5-9 March 2000.

[11] Wilkie W, et al. Reliability Testing of NASA Piezocomposite Actuators. Proc. Actuator 2002 – 8th Int. Conf. on New Actuators, Bremen, Germany, 2002.

[12] Wilkie W, et al. Method of Fabricating a Piezoelectric Composite Apparatus. US Patent No. 6,629,341, 2003.

[13] High J, Wilkie W. Method of Fabricating NASA-Standard Macro-Fiber Piezocomposite Actuators. NASA/TM-2003-212427, ARL TR 2833, 2003.

[14] Wilkie W. NASA MFC Piezocomposites: A Development History. Int. Symp. on Macro Fiber Composite Applications ISMA, Volkswagen "Transparent Factory", Dresden, Germany, 27-28 September 2005.

[15] Wierach P. Piezoceramic Surface Actuator and Method for the Production thereof. Patent No. WO 2008/025315 A1, 2008.

[16] Wierach P, Goetting H C, Schönecker A. Development of Encapsulated PZT-Patches for Adaptive Structures. Adaptronic Congress, Potsdam, Germany, 2000. p. 91-95.

[17] Wierach P. Entwicklung Multifunktionaler Werkstoffsysteme mit piezokeramischen Folien im Leitprojekt Adaptronik. DLR/Inst. for Structural Mechanics, Report, Braunschweig, Germany, 2003.

[18] Williams R B, Inman D J. An Overview of Composite Actuators with Piezoceramic Fibers. Proc. 20th Int. Modal Analysis Conference, Los Angeles, CA, 2002.

[19] Wierach P, Schönecker A. Bauweisen und Anwendungen von Piezokompositen in der Adaptronik. Adaptronic Congress, Göttingen, Germany, 2005.

[20] Pretorius J, Hugo M, Spangler R. A Comparison of Packaged Piezoactuators for Industrial Applications. Smart Structures and Materials 2004: Industrial and Commercial Applications of Smart Structures Technologies, Proc. of the SPIE, Vol. 5388, 2004. p. 131-142.

[21] Melnykowycz1 M, Kornmann X, Huber C, Barbezat M, Brunner A J. Performance of integrated active fiber composites in fiber reinforced epoxy laminates. Smart Mater. Struct. 2006; 15: 204-212.

[22] Hufenbach W, Gude M, Heber T. Design and testing of novel piezoceramic modules for adaptive thermoplastic composite structures. Smart Mater. Struct. 2009; 18: 045012 (7pp).

[23] Hufenbach W, Gude M, Heber T. Development of novel piezoceramic modules for adaptive thermoplastic composite structures capable for series production. Sensors and Actuators A 2009; 156: 22-27.

[24] Hufenbach W, Gude M, Modler N, Heber T, Tyczynski T. Sensitivity analysis for the process integrated online polarization of piezoceramic modules in thermoplastic composites. Smart Mater. Struct. 2010; 19: 105022 (6pp).

[25] Crawley E F, Anderson E H. Detailed Models of Piezoceramic Actuation of Beams. Journal of Intelligent Material Systems and Structures 1990; 1: 4-25.

Figure captions

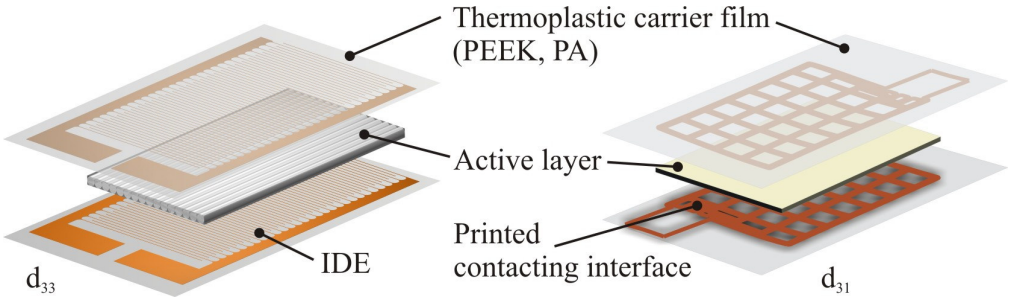

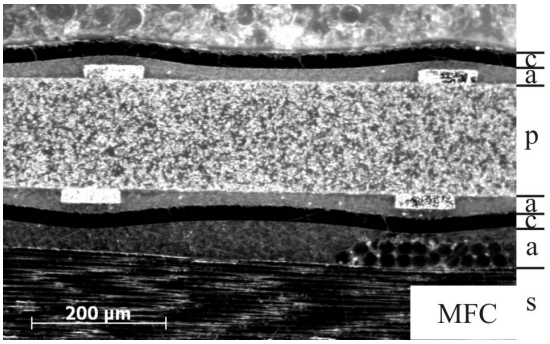

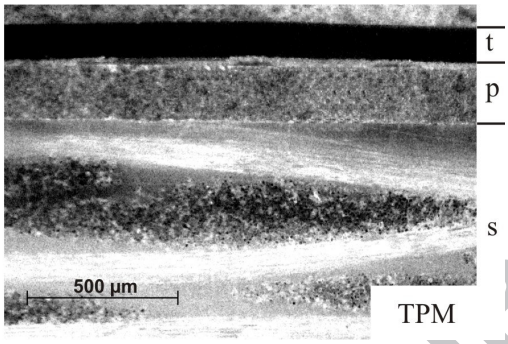

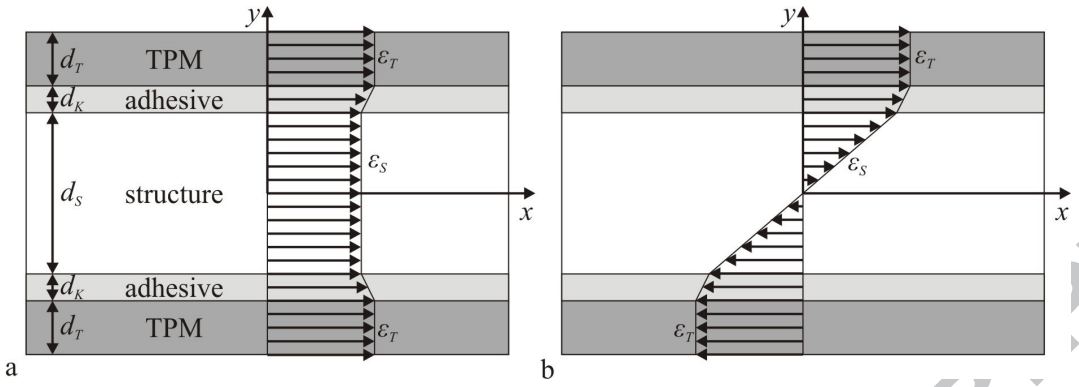

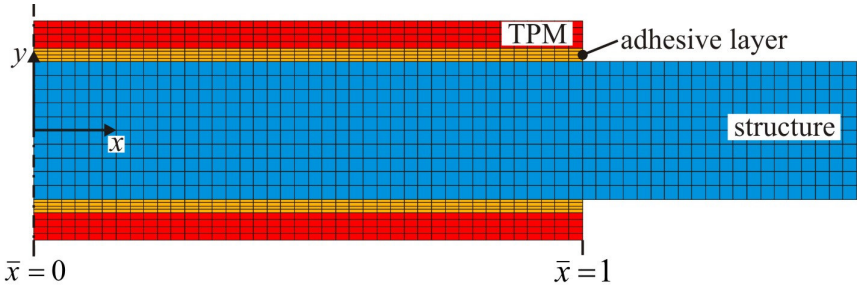

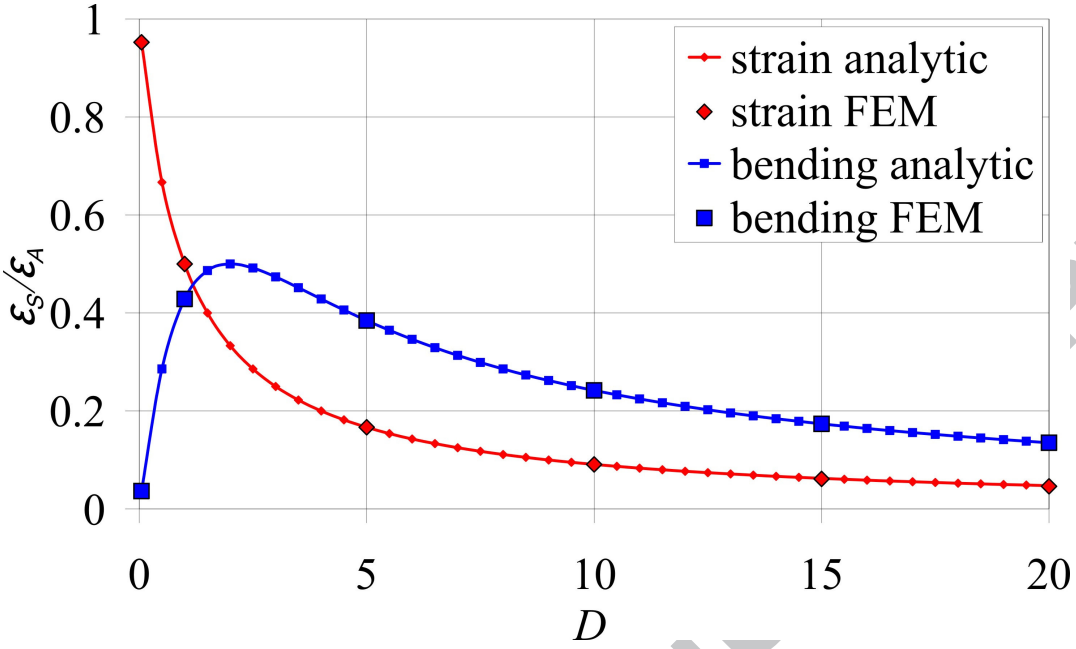

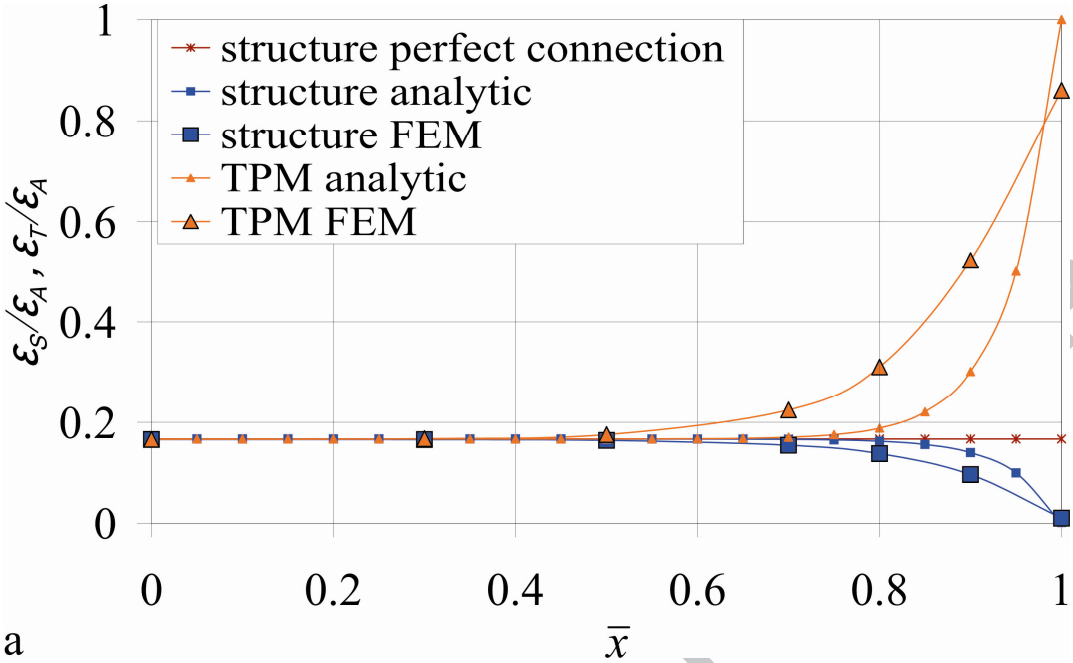

a

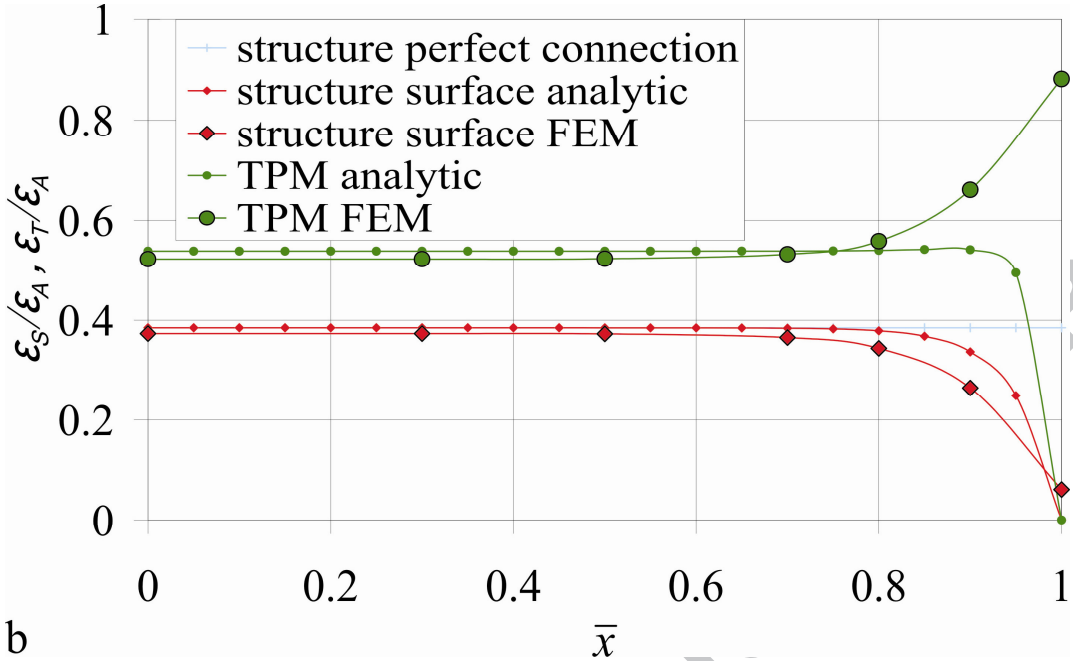

b

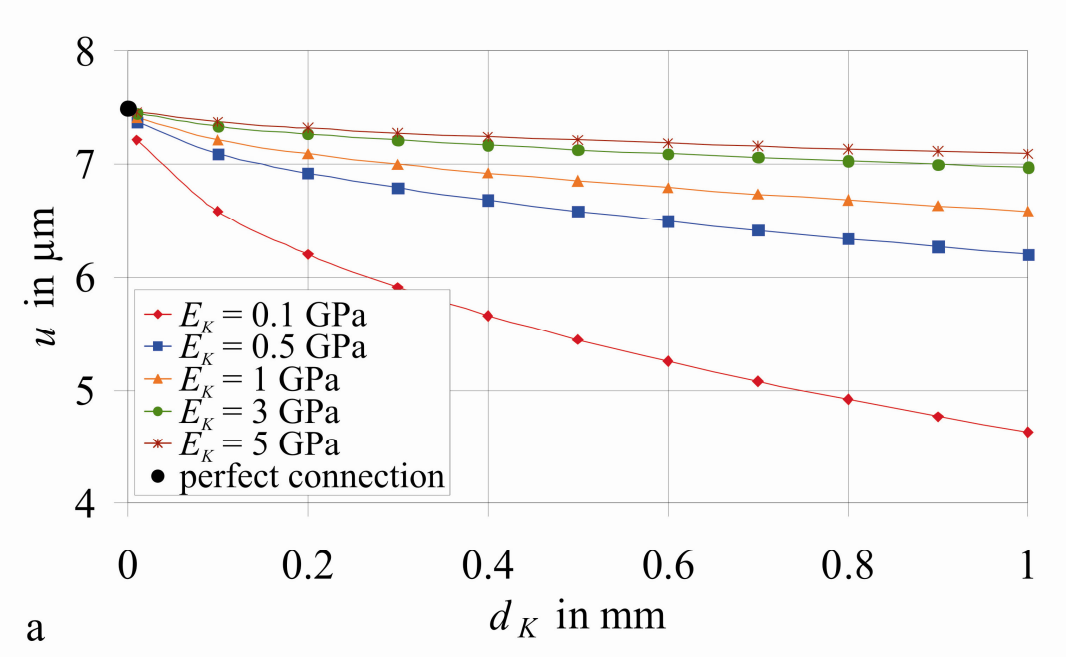

a

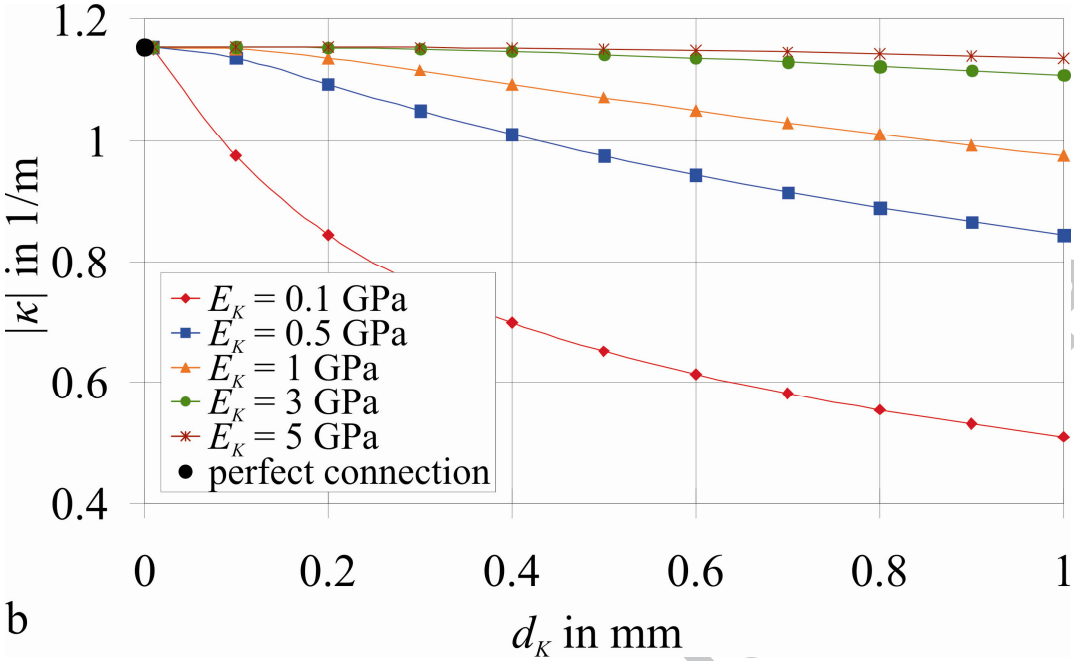

b

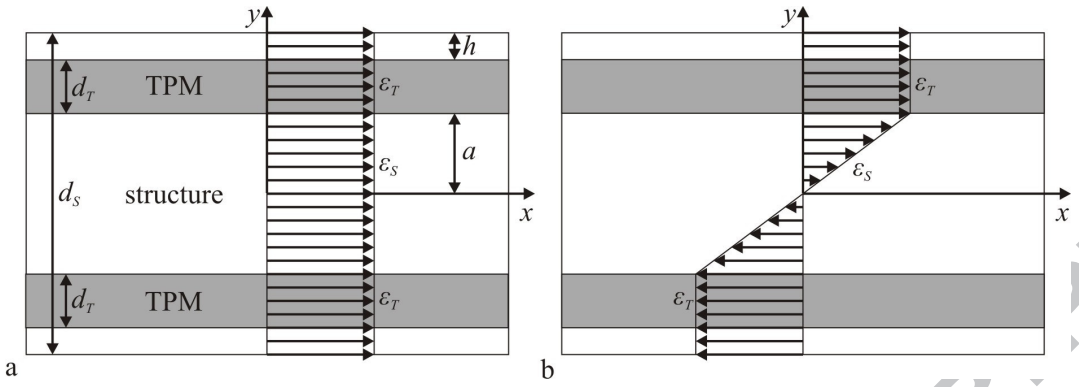

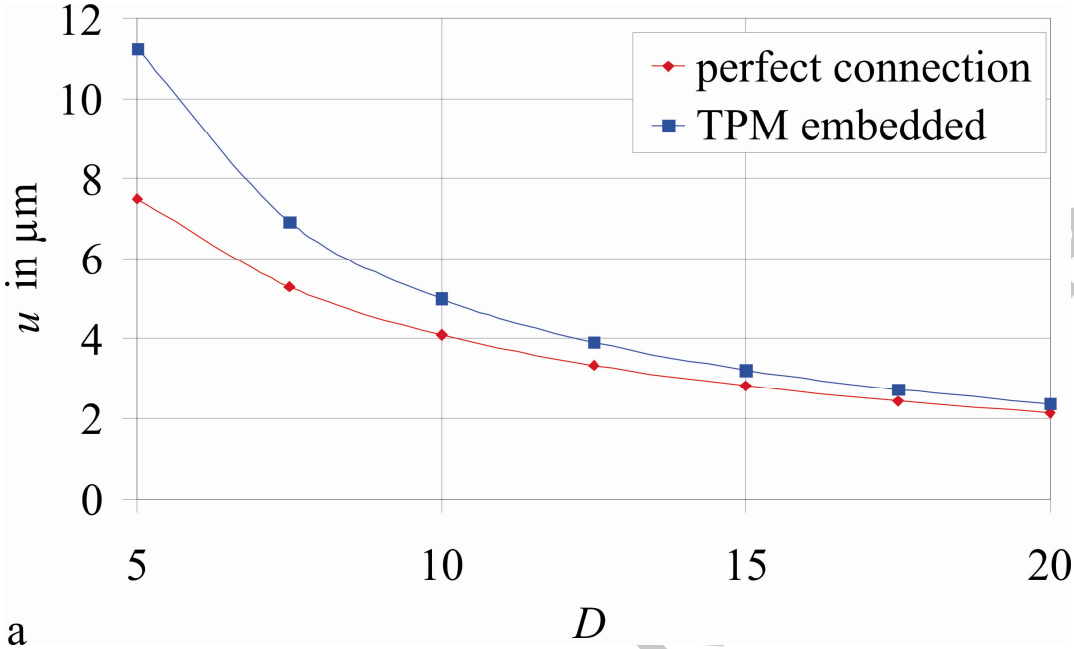

a

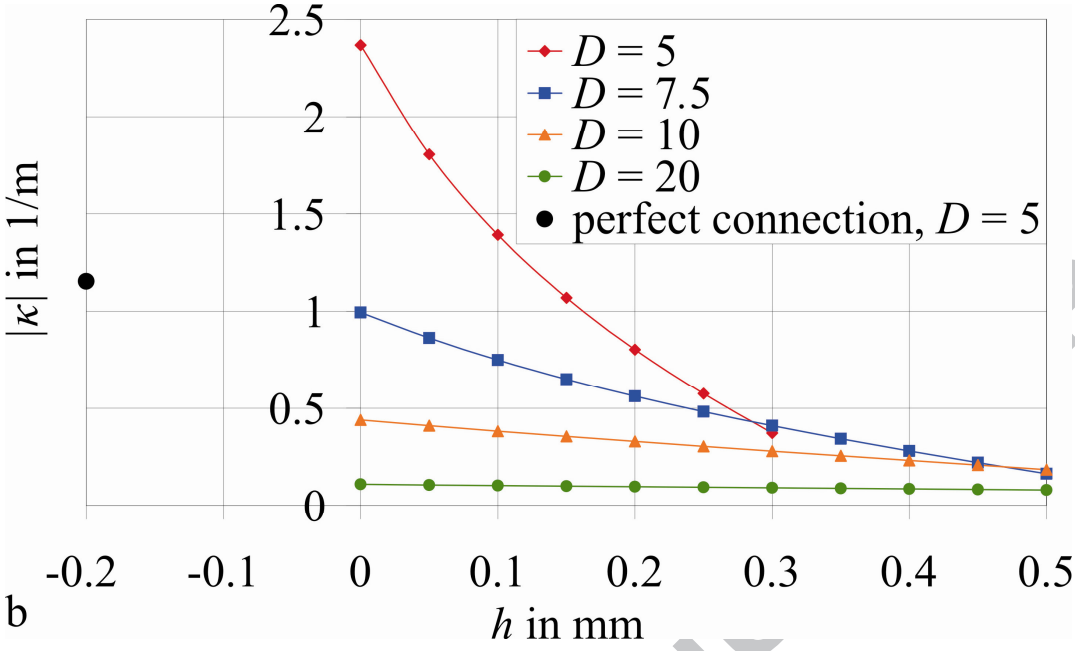

b

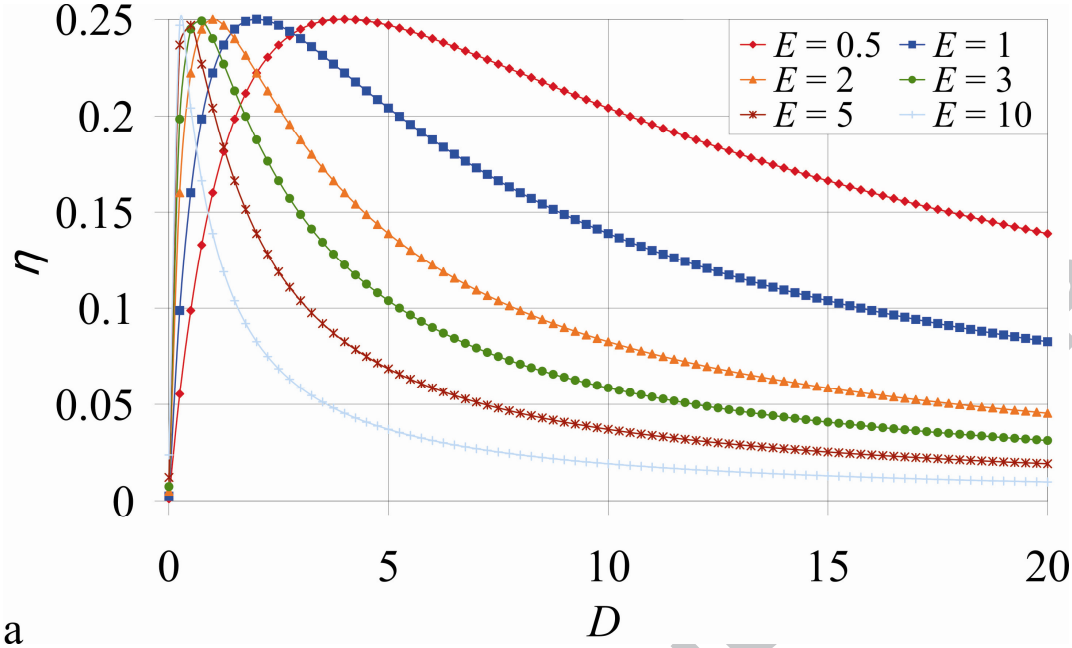

a

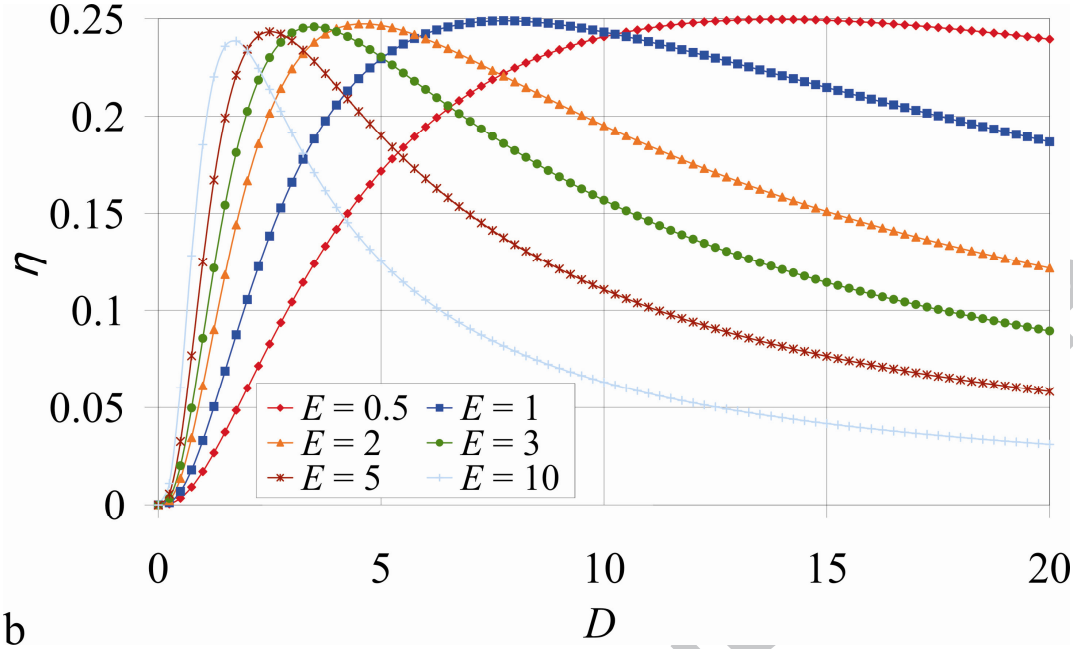

b